Supporting information: Surface recombinations in III-nitride micro-LEDs probed by photon-correlation cathodoluminescence

Sylvain Finot,[†] Corentin Le Maoult,[‡] Etienne Gheeraert,[†] David Vaufrey,[‡] and Gwénolé Jacopin[*,†]

[†] *Univ. Grenoble Alpes, CNRS, Grenoble INP*, Institut Néel, 38000 Grenoble, France*

[‡] *Univ. Grenoble Alpes, CEA, LETI, F-38000 Grenoble, France*

E-mail: gwenole.jacopin@neel.cnrs.fr

I Additional CL measurements

I.1 Effect of the acceleration voltage on spectra

Figure S1 shows room temperature spectra acquired in the middle of a 100 x 100 µm^2 mesa for different acceleration voltages.

At low acceleration voltages, typically below 6 kV, the luminescence of the MQW is not visible. Only the broad blue line (BL) of the *p*-GaN, running from about 390 to 500 nm and the GaN near band edge emission (NBE) at 364 nm can be clearly identified. Additionnally, a weak emission around 380 nm, attributed to electron to acceptor transitions in the *p*-GaN is visible. This band is better resolved at slightly higher acceleration voltage, with the intensity of the broad BL band decreasing in favour of the thinner MQW emission.

Above 7 kV, the MQW intensity centred at 443 nm rapidly increases with the acceleration voltage. Note that at 10 kV, a peak appears at 369 nm, associated with the NBE emission of the n-GaN buffer. As the acceleration voltage increases, the broad yellow band (YB) at 560 nm increases and the p-GaN NBE is replaced by the n-GaN NBE.

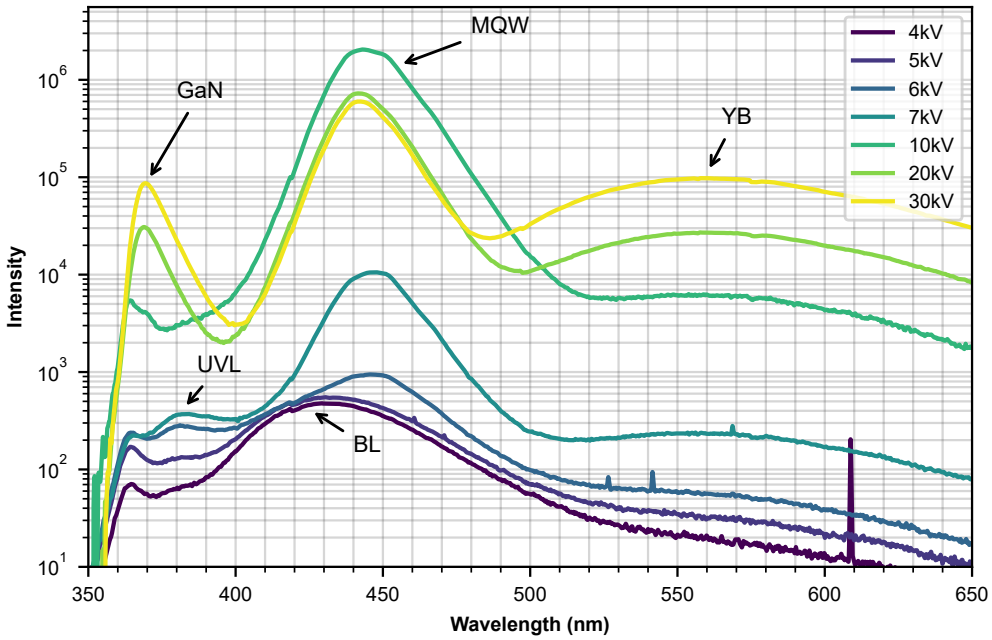

Figure S1: Room temperature spectra acquired in the center of a 100x100 µm^2 mesa for different acceleration voltages

I.2 CL fluctuations in bulk

Figure S2 shows a 10 kV CL image at the quantum well energy acquired in the center of a 2 × 2 mm^2 mesa. We can observe intensity fluctuations with a typical length comparable to the one observed in the etched mesas.

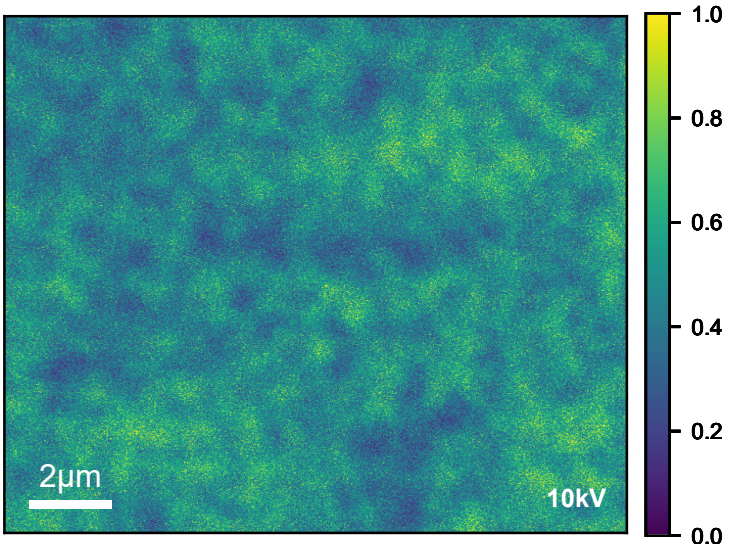

Figure S2: CL image at the quantum well energy (440 ± 10 nm) in the middle of a 2x2 mm^2 mesa

II Nextnano simulations

As shown on Figure S3, we simulated a 1 µm wide mesa, constrained on GaN and surrounded by air to allow strain relaxation. From bottom to top, the simulated structure consists of a thin GaN buffer which imposes the strain, a 200 nm n-GaN layer followed by five 3 nm thick $In_{15}Ga_{85}N$ quantum wells. The GaN barriers are 15 nm thick. After the last barrier, there is a 15 nm $Al_{15}Ga_{85}N$ electron blocking layer. Finally, there is a 180 nm GaN layer. The entire structure is n-doped with a doping level of $10^{17}\,cm^{-3}$.

The calculation scheme in nextnano is as follows, first, the strain is minimized. Then the new band structure taking into account the strain is calculated. Finally, the Schrödinger equation is solved at different positions for both electrons, using the effective mass model, and for holes using a 6×6 kp model. The parameters used can be found in Vurgaftman *et al.*[1]

Figure S4 (a) shows the normalized electron-hole (e-h)) wavefunction spatial overlap defined in (1) as a function of the distance to the edge for the different quantum wells. On average, the variation is contained within a 20 % interval, however, the overlap of the first

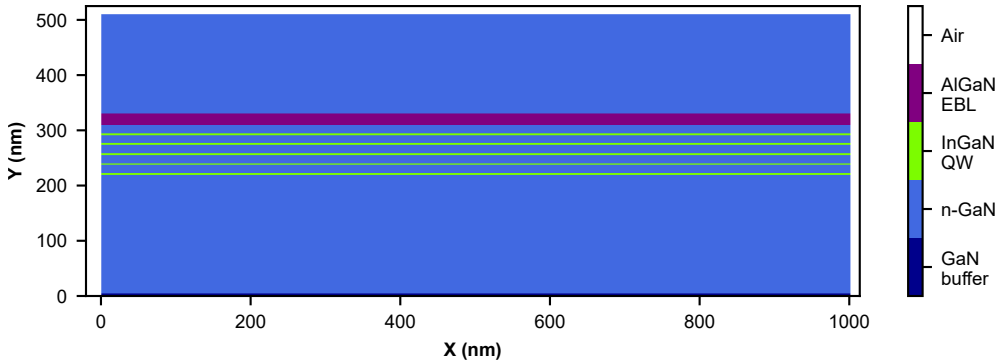

Figure S3: Schematic of the simulated structure

QW, *i.e.* the furthest from the top surface, drops drastically in the vicinity of the edge. The energy shift, defined as the difference between the bulk energy and the energy at a given position is shown on Figure S4 (b). This shift is maximal at the edge position, ranging from + 22 meV to - 16 meV depending on the QW. Note that, experimentally, no shift has been observed.

$$\text{Norm. spatial overlap} = \frac{|\langle \Psi_{hl}(x) | \Psi_{el}(x) \rangle|^2}{|\langle \Psi_{hl,bulk} | \Psi_{el,bulk} \rangle|^2} \tag{1}$$

$$\text{Energy shift} = E_{bulk} - E(x) \tag{2}$$

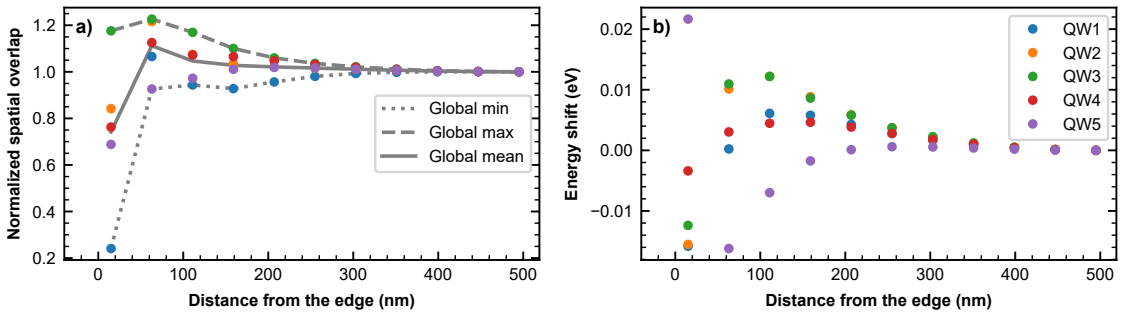

Figure S4: Normalized e-h wavefunction overlap (a) and energy shift (b) for the 5 QWs as a function of the distance to the edge

III Diffusion simulations

The 1D diffusion model we used is based on the diffusion equation (3), where $n(x,t)$ is the local carrier density, D is the ambipolar diffusion coefficient and τ_{eff} the bulk effective lifetime. It is important to note that in our case we assume that τ_{eff} does not depend on the carrier concentration, see justification below (section IV). Additionally, adapted boundary conditions (4) are set to take into account the surface recombination velocity S. An initial carrier concentration profile, following a gaussian distribution centered at the excitation position x_0, with a standard deviation of 150 nm is generated. Then, the model is numerically integrated both in space and time by finite differences.

$$\begin{cases} \dfrac{dn}{dt} = D\left(\dfrac{\partial^2 n}{\partial x^2}\right) - \dfrac{n}{\tau_{eff}} & (3) \\ D\left(\dfrac{dn}{dx}\right)_{x=0} = Sn(x=0) & (4) \end{cases}$$

With this model, for a given excitation position x_0, we obtain for each time step the carrier density profile over the whole sample. We extract a lifetime by fitting the decay of the carrier density integrated over the whole simulation domain N to a stretched exponential

$$N(t) = \int n(x,t)dx$$
$$N(t) \propto \exp\left(-(t/\tau_{eff})^{\beta}\right)$$

We have chosen a stretched exponential because the decay of the carrier density depends on the diffusion and is therefore not constant in time. Indeed, for carriers generated near the edge, the decay is faster at the beginning because they are exposed to surface recombination and slower afterwards, because some of them diffuse away from the edge ($\beta/\beta_{bulk} < 1$). On the contrary, for carriers generated at a certain distance from the edge, initially no carriers are close to the edge, the decay rate increases with time as the carriers start to reach the

edge due to diffusion ($\beta/\beta_{bulk} > 1$) (*cf* Figure S5 (a) and (b)).

The trend observed in the simulations is also seen in the experimental data Figure S5 (b). However, we note that even at a distance of 5 µm to the edge the stretching parameter is not equal to 1. This is probably due to the role of carrier localization in the recombination carrier dynamics.[2]

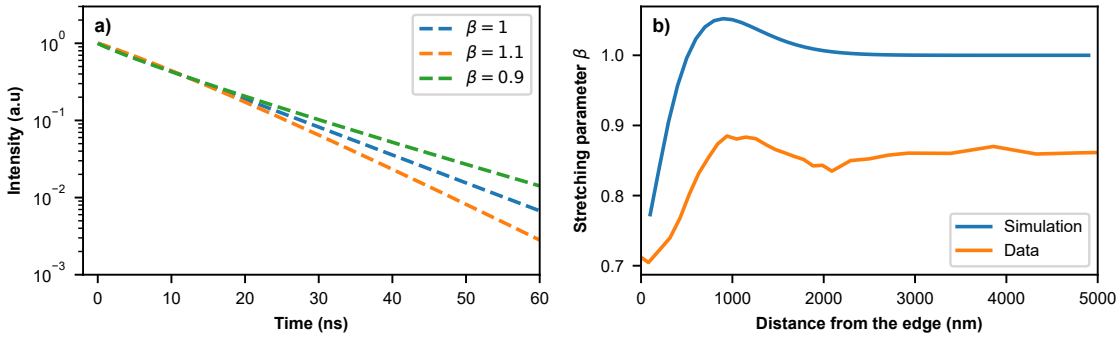

Figure S5: (a) Stretched exponential decay for different stretching parameter. (b) Stretching parameter as a function of the distance to the edge for simulation and experimental data.

On Figure S6 the role of the ambipolar diffusion coefficient D and the surface recombination velocity S are more clearly exposed. It can be seen from Figure S6(a) and (b) that D mainly governs the lateral extension of the affected area, while S is responsible for the decrease of the lifetime in the affected area.

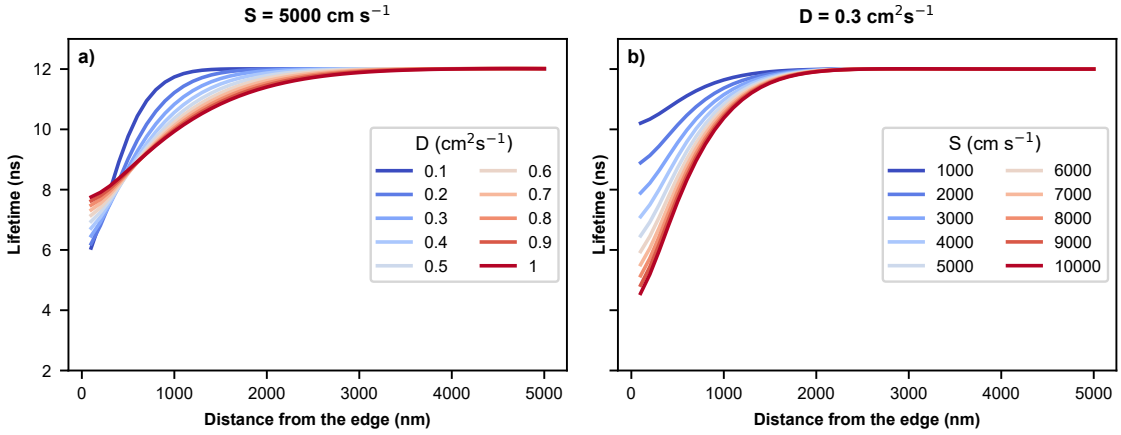

Figure S6: Lifetime profile as a function of the distance from the edge for (a) different value of D and a fixed S and (b) a fixed D and different value of S.

III.1 Influence of the e-h wavefunction overlap

The results presented in the paper assumed a constant lifetime $\tau_{eff}(x) \approx 12\,\text{ns}$. Here, as the lifetime should vary with the e-h wavefunction spatial overlap, we tried to use the spatial overlap calculated with nextnano3 (*cf* Figure S4 (a)) as an input for the simulation. Basically we replaced the effective lifetime τ_{eff} with :

$$\tau_{eff}(x) = \frac{|\langle \Psi_{hl,bulk} | \Psi_{el,bulk} \rangle|^2}{|\langle \Psi_{hl}(x) | \Psi_{el}(x) \rangle|^2} \times \tau_{eff,bulk}$$

As the spatial overlap did not follow the same trend in all quantum wells, we have chosen to compute only the extreme cases indicated on Figure S4 as global max, global min and global mean which correspond respectively to the max, min and mean of the 5 quantum wells' e-h overlap at each position. The corresponding lifetime profiles are shown on Figure S7 (a). Note that as the nextnano3 simulation was only 1 µm wide, the overlap is calculated only on the first 500 nm (*i.e.* from the edge to the center of the mesa). Thus, normalized e-h wavefunction spatial overlaps are set to 1 for distances greater than 500 nm.

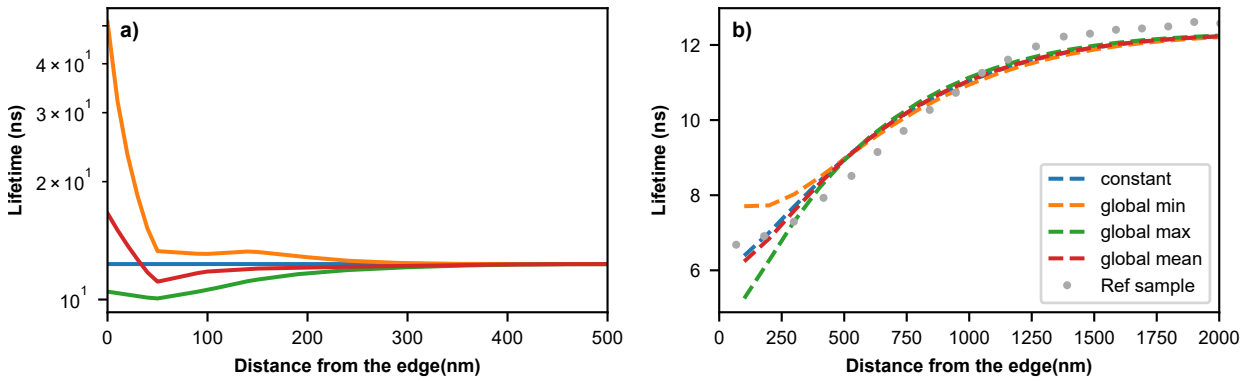

Figure S7: (a) Lifetime profile taking into account the e-h wavefunction spatial overlap calculated with nextnano3. (b) Diffusion model for various lifetime profiles with $D = 0.35\,\text{cm}^2\,\text{s}^{-1}$ and $S = 4750\,\text{cm}\,\text{s}^{-1}$

Figure S7 (b) shows results of the diffusion model for various lifetime profile (see Figure S7 (a)). Even when the lifetime is set to 50 ns near the edge (orange line), the corre-

sponding lifetime profile obtained by fitting the carrier density with the stretched exponential only changes by about 1.5 ns, showing that non-radiative surface recombination prevails over change in radiative lifetime.

III.2 IQE estimation using radial simulations

From our experimental results, we deduce the diffusion coefficient D and surface recombination velocities S for standard µLEDs. It is interesting now to see how the non-radiative surface recombinations affect the efficiency of electrically injected µLEDs.

For simplicity, we considered now, cylindrical devices in the steady state. In theses conditions, the model is defined with the two equations :

$$\begin{cases} D\left(\frac{\partial^2 n}{\partial r^2} + \frac{1}{r}\frac{\partial n}{\partial r}\right) - \frac{n}{\tau_{eff}} = 0 & (5) \\ D\left(\frac{dn}{dr}\right)_{r=d/2} = Sn & (6) \end{cases}$$

where d is the µLED diameter. In this case, the problem can be solved analytically and it is possible to define an effective recombination lifetime $\tau_{eff,\mu LED}$ that takes into account non-radiative surface recombinations and thus reflects the change in IQE induced by sidewall recombinations.[3]

$$\frac{1}{\tau_{eff,\mu LED}} = \frac{4D\beta^2}{d} + \frac{1}{\tau_{eff,bulk}} \quad (7)$$

where β is the solution of the equation:

$$\beta \cdot J_1(\beta) - L \cdot J_0(\beta) = 0 \quad (8)$$

With J_0, the Bessel function of the first kind of order zero and J_1, the Bessel function of the first kind of first order.

The simulations results are displayed in Figure S8. First, in Figure S8(a), we set the

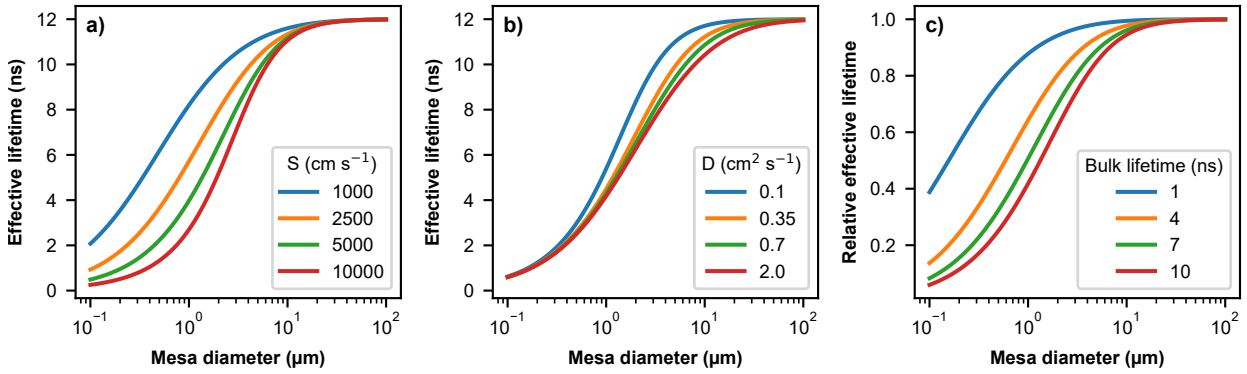

Figure S8: Radial diffusion simulations showing the impact of (a) the surface recombination velocity, (b) the ambipolar diffusion coefficient and (c) the bulk lifetime.

diffusion coefficient $D = 0.35\,\mathrm{cm^2\,s^{-1}}$ and the bulk lifetime to 12 ns. We observe that the effective lifetime and thus the IQE remains unaffected by sidewall recombinations for diameter above 10 µm. However, below this limit, the IQE drops drastically. For small diameter, the IQE can be partially recovered if the surface recombination velocity is reduced.

In Figure S8(b), we set the recombination velocity to $S = 4000\,\mathrm{cm\,s^{-1}}$ and the bulk lifetime to 12 ns. In this case, we vary the diffusion coefficient from 0.1 to $2\,\mathrm{cm^2\,s^{-1}}$. We observe that by reducing the coefficient diffusion to $0.1\,\mathrm{cm^2\,s^{-1}}$, it is possible to maintain a good IQE for µLEDs with diameter of 3 µm.

Finally, in Figure S8(c), we investigate the influence of the bulk effective lifetime. In this case, the recombination velocity is set to $S = 4000\,\mathrm{cm\ s^{-1}}$ and the diffusion coefficient to $D = 0.35\,\mathrm{cm^2 s^{-1}}$. Thus, by increasing the recombination rate by one order of magnitude, it is possible to maintain the bulk IQE value for µLEDs with a diameter down to 2 µm.

IV Carrier density independent lifetime

By performing additional CASINO simulation, we could estimate the interaction volume. By taking as a criterion the volume where 90% of the interaction occurs, we estimate the volume V (see Figure S9).

$$V = \frac{4\pi}{3} R_Z R_L^2 = \frac{4\pi}{3} \left(2.2 \times 10^{-5}\right)^2 \left(2.7 \times 10^{-5}\right) \approx 5.5 \times 10^{-14}\,\mathrm{cm}^{-3}$$

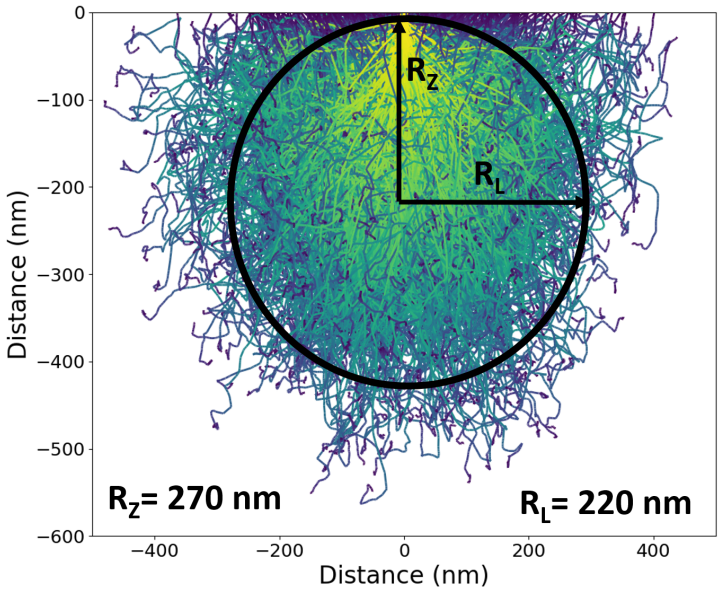

Figure S9: Generation volume of a 10 kV electron beam in GaN

In the volume, the number of electron-hole pairs generated per incident electron in the sample can be approximated by[4] :

$$N_{e-h} \approx (1-f)\frac{E_b}{3E_G} = (1-0.24)\frac{10000}{3 \times 3.4} \approx 750\,\text{e-h pairs}$$

Where f is the backscattered coefficient, E_b is the acceleration voltage and E_G is the bandgap. Thus, right after the electron to e/h pair process, the maximum carrier density in our system is around:

$$n = \frac{N_{e-h}}{V} \approx 1.3 \times 10^{16}\,\mathrm{cm}^{-3}$$

We can thus estimate the contribution of radiative and Auger recombinations, through

the ABC model.

$$R = An + Bn^2 + Cn^3 = \frac{n}{\tau_{eff}} \approx \frac{1.3 \times 10^{16}\,\mathrm{cm}^{-3}}{12\,\mathrm{ns}} \approx 1.1 \times 10^{24}\,\mathrm{cm}^{-3}\,\mathrm{s}^{-1}$$

According to A. David *et al.*,[5] for a LED emitting at 440 nm, both radiative and Auger recombination coefficient are below:

$$B < 1 \times 10^{10}\,\mathrm{cm}^3\,\mathrm{s}^{-1} \text{ and } C < 1 \times 10^{-29}\,\mathrm{cm}^6\,\mathrm{s}^{-1}$$

Thus, we can estimate an upper value to the contribution of the radiative and Auger terms to the recombination rate:

$$Bn^2 < 1.7 \times 10^{22}\,\mathrm{cm}^{-3}\,\mathrm{s}^{-1},\ Cn^3 < 2 \times 10^{19}\,\mathrm{cm}^{-3}\,\mathrm{s}^{-1} \ll\ R \approx 1.1 \times 10^{24}\,\mathrm{cm}^{-3}\,\mathrm{s}^{-1}$$

Therefore, given the low excitation density of our measurements, the carrier dynamics is simply governed by the equation:

$$-\frac{dn}{dt} = An$$

For this reason, in our simulation, we considered a carrier independent effective lifetime.

References

(1) Vurgaftman, I.; Meyer, J. R. Band parameters for nitrogen-containing semiconductors. *Journal of Applied Physics* **2003**, *94*, 3675–3696.

(2) Pophristic, M.; Long, F. H.; Tran, C. A.; Ferguson, I. T. Time-Resolved Photoluminescence Measurements of InGaN Light-Emitting Diodes. *Materials Science Forum* **2000**, *338-342*, 1623–1626.

(3) Daiminger, F. X.; Schmidt, A.; Faller, F.; Forchel, A. W. B. Picosecond time-resolved

investigations of carrier lifetime and carrier capture in InGaAs/GaAs quantum dots. Quantum Well and Superlattice Physics V. 1994; pp 213–221.

(4) Tchernycheva, M.; Jacopin, G.; Piazza, V. *Fundamental Properties of Semiconductor Nanowires*; Springer, 2021; pp 251–288.

(5) David, A.; Young, N. G.; Lund, C.; Craven, M. D. Review—The Physics of Recombinations in III-Nitride Emitters. *ECS Journal of Solid State Science and Technology* **2020**, *9*, 016021.